



OPEN ACCESS

EDITED BY

Nuria Álvarez-Sánchez,
University of Toronto, Canada

REVIEWED BY

Daliya Banerjee,
Independent Researcher, Boston, MA,
United States
Bennie Van Heeswijk,
Erasmus Medical Center, Netherlands

*CORRESPONDENCE

Remy Robert

✉ remy.robert@monash.edu

RECEIVED 20 October 2025

REVISED 03 December 2025

ACCEPTED 09 December 2025

PUBLISHED 09 January 2026

CORRECTED 14 January 2026

CITATION

Alam MJ, Yap Y-A, Ang C, Xie L, Shane HL,
Mackay CR and Robert R (2026) Fc-enhanced
anti-CCR6 antibody elicits robust therapeutic
effects across multiple autoimmune diseases.
Front. Immunol. 16:1728419.
doi: 10.3389/fimmu.2025.1728419

COPYRIGHT

© 2026 Alam, Yap, Ang, Xie, Shane, Mackay
and Robert. This is an open-access article
distributed under the terms of the [Creative
Commons Attribution License \(CC BY\)](#). The
use, distribution or reproduction in other
forums is permitted, provided the original
author(s) and the copyright owner(s) are
credited and that the original publication in
this journal is cited, in accordance with
accepted academic practice. No use,
distribution or reproduction is permitted
which does not comply with these terms.

Fc-enhanced anti-CCR6 antibody elicits robust therapeutic effects across multiple autoimmune diseases

Md Jahangir Alam ¹, Yu-Anne Yap¹, Caroline Ang¹, Liang Xie²,
Hillary L. Shane³, Charles R. Mackay ² and Remy Robert ^{1*}

¹Department of Physiology, Biomedicine Discovery Institute, Monash University, Clayton,
VIC, Australia, ²Department of Microbiology, Biomedicine Discovery Institute, Monash University,
Clayton, VIC, Australia, ³Dragonfly Therapeutics, Waltham, MA, United States

Activation of the chemokine receptor CCR6 orchestrates the trafficking of IL-17-producing pathogenic immune cells to the sites of inflammation, thus contributing to the development of numerous inflammatory and autoimmune diseases. As such, CCR6 has emerged as a promising therapeutic target for treating Th17-mediated inflammatory disorders. In this study, we employed a targeted strategy, which we termed ‘immunological surgery’, using an Fc-engineered anti-human CCR6 monoclonal antibody (α hCCR6 DLE-mut mAb) designed to engage effector mechanisms against CCR6⁺ immune cells and deplete them. We evaluated the therapeutic efficacy of this approach in preclinical mouse models of representative autoimmune conditions, including scleroderma, psoriasis, and rheumatoid arthritis. Selective targeting of CCR6⁺ cells with α hCCR6 DLE-mut mAb exhibited remarkable efficacy in reducing established inflammation across all disease models. In a bleomycin-induced scleroderma model, α hCCR6 mAb treatment markedly reduced dermal thickening and attenuated scleroderma-associated lung inflammation and fibrosis. In the imiquimod-induced psoriasis model, administration of α hCCR6 mAb led to significant reductions in skin thickening, epidermal hyperplasia, and dermal immune cell infiltration. Similarly, in the collagen-induced arthritis (CIA) model, α hCCR6 mAb treatment significantly alleviated all signs of joint inflammation. Thus, our findings demonstrated that CCR6-targeted therapy could be a promising and effective approach for the treatment of Th17-mediated inflammatory disorders. Moreover, we believe this approach may overcome the challenge of chemokine receptor redundancy by leveraging receptor-specific signatures to eliminate pathogenic leukocyte subsets with high precision.

KEYWORDS

arthritis, CCR6, IL-17A, inflammation, monoclonal antibody (mAb), psoriasis, scleroderma, Th17 cells

1 Introduction

The migration of leukocytes to inflammation sites in response to various chemotactic stimuli allows the immune system to fight an aggression, defend against invading pathogens, and maintain normal homeostasis. While this process is essential for host defense and immune homeostasis, an excessive or chronic influx of immune cells into specific tissues can lead to various immune-mediated inflammatory pathologies, such as autoimmune diseases and chronic inflammatory disorders. Consequently, the selective targeting of chemokine receptors to inhibit the migration of rogue immune cells has been considered an attractive therapeutic strategy to treat inflammation associated with inflammatory and autoimmune diseases.

For instance, the chemokine receptor CCR6, which is predominantly expressed on IL-17 and IL-22-producing T-cells, including Th17 cells (1, 2) and subsets of B-cells (3, 4), has been implicated in numerous inflammatory and autoimmune conditions and facilitates the migration of pathogenic immune cells to the sites of inflammation (5–7). In murine models of psoriasis, a distinct immune cell population expressing low levels of $\gamma\delta$ T-cell receptor (TCR $\gamma\delta$) and high levels of CCR6 serves as a significant source of IL-17 (8–11), contributing to the initiation and maintenance of skin inflammation (10, 12, 13). Similarly, in humans, dermal $\gamma\delta$ T cells secrete IL-17, which plays a critically pathogenic role in skin inflammatory reactions (8).

In systemic sclerosis, both Th17 cells and IL-17 have been implicated in disease progression and fibrosis in mouse models (14, 15), and IL-17^{-/-} mice exhibit resistance to the disease (15). Elevated levels of Th17 cells and IL-17 have been observed in patients with scleroderma (16–20). Moreover, IL-17 has been shown to promote fibroblast activation and collagen production in scleroderma patients (21), further supporting its critical involvement with the development of fibrosis.

In rheumatoid arthritis (RA) patients, CCR6⁺ cells are elevated in the inflamed synovium and peripheral blood (22–24). In RA joints, myeloid cells exhibit increased secretion of CCL20 and facilitate the recruitment of CCR6⁺ Th17 cells, thereby sustaining joint inflammation (1). Fibroblast-like synoviocytes also produce CCL20, further contributing to local inflammation by attracting Th17 cells into the synovium (25).

The pathogenic role of CCR6 has been validated in multiple preclinical models of autoimmune and inflammatory disorders, through genetic deletion or pharmacological blockade (10, 26–28). Previously, we and others have shown that CCR6 blockade using mAbs and/or small molecules was effective in treating psoriasis and experimental autoimmune encephalomyelitis (EAE) (1, 13). However, despite the well-documented involvement of chemokine receptors in many inflammatory diseases, the redundancy of the chemokine system has been thought to be a major reason for the failure of drug development in this area. To overcome this challenge, we developed a novel therapeutic strategy based on the targeting of CCR6⁺ cells using a Fc-engineered anti-human CCR6 mAb (α hCCR6 DLE-mut mAb). This approach, which we term ‘immunological surgery’, is designed to engage Fc-

dependent effector functions against pathogenic immune subsets defined by their chemokine receptor expression, rather than merely blocking receptor signaling. We evaluated the efficacy of α hCCR6 DLE-mut mAb in human CCR6 knock-in (hCCR6 KI) mice across three representative models of IL-17-driven autoimmunity: bleomycin-induced scleroderma, imiquimod-induced psoriasis, and collagen-induced arthritis (CIA). Given the central role of CCR6 in mediating the migration and effector functions of IL-17-producing Th17 cells, we hypothesized that targeting CCR6⁺ cells using Fc-enhanced mAb would yield broad therapeutic benefit across multiple autoimmune contexts.

Our results demonstrate that treatment with α hCCR6 mAb significantly attenuates disease severity and immune cell infiltration in all three models, highlighting the potential of this CCR6-targeting Fc-enhanced antibody strategy as a promising and viable immunotherapy with translational relevance across multiple autoimmune disease contexts. Moreover, this approach could be potentially extended to other chemokine receptor signatures for the targeted depletion of specific pathogenic cell subsets through antibody-mediated interventions and may overcome the limitations posed by chemokine system redundancy in drug development.

2 Materials and methods

2.1 Mice

Human CCR6 knock-in (hCCR6-Tg/mCCR6^{-/-}) mice on a C57BL/6 background were generated using CRISPR/Cas9-based protocol as previously reported (29). hCCR6-Tg/mCCR6^{-/-} female mice between 8 and 10 weeks of age were obtained from the Monash Animal Research Platform, Monash University, Victoria, Australia. Mice were maintained under specific pathogen-free conditions on a 12/12-hour light/dark cycle and had free access to food and water. All animal care and experimental procedures used in this study were approved by the Animal Ethics Committee of Monash University.

2.2 Generation and engineering of α hCCR6 mAb

The α hCCR6 mAb (clone# 6H12) used throughout this study was isolated and humanized as previously described (13). The α hCXCR2 antibody (clone# TAHX2) was used as an isotype control (30).

To produce the DLE depleting variants (DLE Fc- S239D/A330L/I332E) human IgG1, standard mutagenesis techniques were used. The DLE mutations increase the affinity of the Fc for both human and mouse Fc γ R and thus increase ADCC and ADCP activities. The sequences were confirmed on both strands by DNA sequencing.

The variable genes were amplified by PCR and cloned into a mammalian expression vector containing the human kappa and

human heavy chain IgG1 Fc DLE constant regions. Recombinant DNA was transfected into CHO-DG44 cells using the AMAXA nucleofactor device (Lonza) according to the manufacturer's protocol. The transfected CHO cells were grown and maintained in a serum-free medium (Invitrogen) for antibody production. The antibodies were purified from the culture supernatant by affinity chromatography on a ProsepvA protein A column (Millipore). The bound mAbs were eluted with 0.2 M glycine/1 M NaCl, pH 3.0 into a neutralizing solution of 1 M Tris, pH 8.0, and then the buffer was exchanged against phosphate-buffered saline (PBS). Purified antibodies were endotoxin-free as determined by a chromogenic LAL assay (GenScript).

2.3 Antibody-dependent cell-mediated cytotoxicity assay

The ADCC activity of α hCCR6 mAbs was assessed by flow cytometry, following established protocols (13, 31). Briefly, hCCR6-expressing L1.2 target cells were labeled with the membrane dye PKH26 to allow discrimination from effector cells during coculture. Labeled target cells were washed 3 times and resuspended at 2×10^6 cells/mL in culture medium and seeded into round-bottom 96-well plates (5×10^4 cells/well in 25 μ L). Cells were preincubated for 30 minutes at 37°C with serial dilutions 1:4, starting from 2 μ g/mL of α hCCR6 DLE-mut, α hCCR6 Fc-Null, or human IgG1 isotype control mAbs.

Human PBMCs were isolated from heparinized whole blood of healthy donors via Ficoll-Paque density gradient centrifugation. NK cells were subsequently isolated using MACS CD56 microbeads and positive selection columns (Miltenyi Biotec), according to the manufacturer's instructions. Purified NK cells (2×10^5 /well) were added to the antibody-treated target cells at an effector-to-target (E:T) ratio of 4:1 and incubated for 3 hours at 37°C in the presence of 10% heat-inactivated human serum. Following incubation, cells were transferred to microtiter tubes containing 10 μ M of TO-PRO-3 iodide (Thermo Fisher Scientific) to identify dead cells. Samples were acquired using a BD FACSymphonyTM flow cytometer and analyzed using FlowJo software v10 (FlowJo, LLC).

2.4 Bleomycin-induced scleroderma

Mice were anaesthetized using 4% isoflurane in 2L/minute of oxygen. The backs of anaesthetized mice were shaved with an electric clipper and then treated with depilatory cream to remove hair. The next day, mice were subcutaneously (s.c.) injected with 100 μ L of Bleomycin (BLM) (Millipore Sigma) solution (1 mg/mL in PBS) at a single location on the shaved backs of mice for 4 weeks using a 27-gauge needle. The exact amount of PBS was injected as a control. Dorsal skin thickness was measured every other day just before s.c. injection of BLM with a digital thickness gauge, and the change in percentage was calculated compared to the thickness on day 0. For the therapeutic regimen, mice were treated with BLM until their dorsal skin thickening (~15%) exhibited symptoms of the

disease and the onset of fibrotic signs (32, 33) (on day 8). A loading dose (25 mg/kg of body weight) of either an α hCCR6 or an isotype control mAbs was administered intraperitoneally (i.p.), followed by maintenance doses (5 mg/kg, i.p.) twice a week. This antibody regimen was chosen based on our published study using an anti-CXCR2 mAb (30). Mice were evaluated daily by an observer blind to the treatment groups. Back skin redness (erythema) and the presence of scales (scaling) of the skin were scored using a semiquantitative scoring system from 0 to 4 based on their external physical appearance: 0 = no skin abnormalities, 1 = slight, 2 = moderate, 3 = marked, and 4 = severe. On day 29, mice were humanely killed by CO₂ asphyxiation at a controlled flow rate of 50% of the chamber volume per minute. Dorsal skin, skin-draining lymph nodes (LNs), spleen, lung, and lung-draining LNs were subsequently harvested for assessment of cellular infiltration and histological analysis.

2.5 Imiquimod-induced psoriasis

Mice were anaesthetized using 4% isoflurane in 2L/minute of oxygen. Their backs were shaved with an electric clipper and then treated with depilatory cream to remove hair. On the next day, 20 mg IMQ cream 5% (Aldara; 3M Pharmaceuticals) or vaseline (as a control cream) was applied daily to the back (dorsal) skin for 7 consecutive days. Dorsal skin thickness was measured every day just before the application of IMQ cream using a digital thickness gauge, and the change in percentage was calculated compared to the thickness on day 0. For the therapeutic regimen, mice were treated with IMQ cream until dorsal skin thickening (~30%) indicated disease progression (on day 3). Mice were then administered a loading dose (25 mg/kg of body weight, i.p.) of either an α hCCR6 or an isotype control (which one), followed by maintenance doses (5 mg/kg, i.p.) every other day for a week. Mice were evaluated daily by an observer blind to the treatment groups. Dorsal skin erythema and scaling were scored using a semiquantitative scoring system from 0 to 4 based on their external physical appearance: 0 = no skin abnormalities, 1 = slight, 2 = moderate, 3 = marked, and 4 = severe. On day 9, mice were humanely killed by CO₂ asphyxiation at a controlled flow rate of 50% of the chamber volume per minute. Following euthanasia, dorsal skin, spleen, and skin-draining LNs were collected for evaluation of cellular infiltration and histological changes.

2.6 Collagen-induced arthritis

Mice were anaesthetized using 4% isoflurane in 2L/minute of oxygen, and immunized s.c. at two sites at the base of the tail with a 100 μ L emulsion of 100 μ g Chicken type II collagen (CII, Sigma) and 200 μ g *Mycobacterium tuberculosis* in Complete Freund's Adjuvant (Chondrex) in equal volumes, as previously described (34). On Day 21 post-immunization, mice were boosted with 100 μ g of CII emulsified with Incomplete Freund's adjuvant (Sigma). Mice were evaluated and scored for arthritis three times a week from Day

18 post-immunization. Arthritis severity was scored on a scale of 0 to 4, as follows: 0 = no evidence of erythema and swelling; 1 = one or two toes inflamed and swollen with no apparent swelling of the paw or ankle; 2 = Three or more toes inflamed and swollen but no paw swelling or mild swelling of entire paw; 3 = swelling of entire paw; and 4 = severe swelling of entire paw or ankylosis of the paw. Arthritis severity was determined as the sum of scores for all four legs. When mice exhibited swelling in ankle joints and front paws with an average cumulative clinical score of 4 (day 41), mice were treated with eight i.p injections of 5 mg/kg of body weight with the α CCR6 or isotype control mAbs, every other day for 3 weeks. On day 60, mice were humanely killed by CO₂ asphyxiation at a controlled flow rate of 50% of the chamber volume per minute. Thereafter, blood, ankle joints, and popliteal draining LNs were harvested for analysis of CII-specific IgG antibodies, cellular infiltration, and histology.

2.7 Histological evaluation and quantification

Following euthanasia through CO₂ asphyxiation, lung, dorsal skin, and ankle samples were excised, collected and fixed in 10% neutral buffered formalin (NBF) for 24 hours. Tissues were processed, followed by paraffin embedding and sectioning at 4 μ m. Lung and skin sections were stained with hematoxylin and eosin (H&E) and evaluated at 20 \times magnification to quantify the dermal thickness using ImageJ software (National Institutes of Health). The percentage of fibrosis in lung tissue sections stained with Masson's trichrome (MT) was quantified using ImageJ software. Lung and skin tissue sections were stained with Picrosirius red (PSR) to determine collagen deposition. MT staining was performed on the skin and lung sections to analyze fibrosis using a numerical fibrosis scoring scale of the modified Ashcroft score (35, 36), a score of 0 was considered as no fibrosis, 1 as minimal, 2 as mild, 3 as moderate, and 4 as severe fibrosis. All sections were scored independently by an investigator in a blinded manner.

For both scleroderma and psoriasis skin tissue sections, the dermal thickness was measured at five different locations on the same slide, and the average value was calculated to represent the findings for each tissue sample. Ankle sections were stained with H&E and Safranin O to examine cell infiltration and cartilage destruction.

2.8 Mouse tissue processing and single-cell preparation

For skin single-cell suspension, dorsal skin pieces were taken from the same anatomical region across animals. We excised a 1.0 \times 1.0 cm full-thickness dorsal skin piece and trimmed subcutaneous fat. Thus, tissue size and weight were similar across animals through uniform anatomical dissection, ensuring comparability of absolute cell counts. Skin samples were minced with scissors and digested

with 0.2 mg/mL of Liberase TL (Roche Diagnostics) and 0.5 mg/mL of DNase (Roche Diagnostics) in RPMI for 1 hour at 37 °C with agitation. After the digestion, the cell suspension and the remaining tissue fragments were passed through a 70 μ m cell strainer and washed with cold RPMI-1640 containing 5 mM EDTA. The cell suspension was filtered through 100 μ m and then 40 μ m nylon mesh filters, and washed with cold FACS buffer (PBS containing 2% FCS and 4 mM EDTA).

For mouse lung single-cell suspensions, lungs were perfused with PBS, minced with scissors in RPMI-1640 medium (Gibco by Life Technologies) with 10% of FCS, and digested with 0.5 mg/mL of Collagenase Type IV (Gibco by Life Technologies) and 1 μ g/mL of DNase I (Roche Diagnostics) for 45 minutes at 37 °C under agitation. After the digestion, the cell suspension and the remaining tissue fragments were passed through a 70 μ m cell strainer and washed with cold RPMI-1640 containing 5 mM of EDTA. Red blood cells were depleted with a lysis buffer and washed with cold PBS. For further purification, cell pellets were resuspended in 4 mL of 40% isotonic Percoll solution and centrifuged at 1000g for 20 mins at room temperature (RT) without using the brake. The cell pellets were then washed with cold PBS.

For single-cell suspensions harvested from the ankle joints, bone marrow cells were initially flushed out using a 27-gauge needle filled with 1 mL RPMI 1640. Ankles were then chopped into 3 to 4 mm chunks and digested with 2.4 mg/mL Hyaluronidase (Sigma) and 1 mg/mL Collagenase Type VIII (Sigma) in RPMI-1640 containing 10% BCS for 1 h at 37°C under agitation. Following digestion, the cell suspension was filtered through a 70 μ m cell strainer and washed with cold FACS buffer to yield a single-cell suspension.

For mouse splenic cell suspensions, spleens were mechanically disrupted in cold PBS and passed through a 70 μ m strainer. Cells were then subjected to red blood cell lysis and washed with cold PBS. For draining LNs, the LNs were mechanically disrupted, passed through a 70 μ m cell strainer, and washed with cold FACS buffer to obtain a single-cell suspension.

2.9 Measurement of anti-CII antibodies

Plasma concentrations of anti-CII autoantibodies (Abs) were measured by ELISA. Briefly, a 96-well microtiter plate (NUNC MaxiSorp) was coated overnight at 4°C with 2 μ g/mL chicken collagen (Sigma) in PBS. The plate was then washed with PBS Tween 0.05% (Amresco) and blocked in 2% BSA in PBS for 1 hour at RT. After incubation, the plates were washed with PBS Tween 0.05%, and diluted standards or plasma samples were added to the wells and incubated at RT for 2 hours. The plates were washed with PBS Tween 0.05% and HRP-conjugated anti-mouse IgG, IgG1, IgG2b or IgG2c (1:1000 dilution in PBS) was added and incubated for 1 hour at RT. TMB substrate (Thermo Scientific) was then added to each well and incubated for 15 mins. After incubation, the reaction was stopped with 0.5M H₂SO₄, and absorbance was measured at 450 nm and 540 nm. The final values were obtained by subtracting the 540 nm readings from

the 450 nm readings. Diluted isotype control pooled plasma samples were used to generate the standard calibration curve, with the highest optical density (OD) value set to 1 arbitrary unit (AU). Data were analyzed using a four-parameter logistic (4PL) function for curve fitting and quantification.

2.10 Flow cytometry

Cells were suspended in FACS buffer and treated with mouse FcR blocking reagent (Miltenyi Biotech) for 10 mins at RT to prevent non-specific antibody binding during cell staining procedures. For myeloid cells analysis in the scleroderma model, cells were stained with surface marker-specific following antibodies in the dark at 4°C for 30 mins: anti-mouse CD45 (clone 30-F11, BD Pharmingen); anti-mouse CD11b (clone M1/70, BD Pharmingen); anti-mouse Ly6G (clone 1A8, BioLegend); anti-mouse Siglec-F (clone E50-2440, BD Pharmingen); anti-mouse CD11c (clone HL3, BD Pharmingen); anti-mouse CD19 (clone 1D3, BD Pharmingen); anti-mouse CD45R (clone RA3-6B2, BD Horizon); anti-mouse PDCA-1 (clone eBio927, eBioscience). Dead cells were excluded using 7-AAD (BD Pharmingen).

For T cell analysis in the scleroderma model, the cells were stained with surface marker-specific following antibodies in the dark at 4°C for 30 mins: anti-mouse CD45 (clone 30-F11, BD Pharmingen), anti-mouse TCR β (clone H57-597, BD Horizon), anti-mouse TCR $\gamma\delta$ (clone GL3, BioLegend), anti-mouse CD4 (clone RM4-5, BD Horizon) and anti-mouse CD8 α (clone 53-6.7, BioLegend), anti-human CCR6 (clone G034E3, BioLegend), anti-mouse Ly6G (clone 1A8, BioLegend), and anti-mouse CD11b (clone M1/70, BD Pharmingen). Dead cells were excluded using 7-AAD (BD Pharmingen).

For the psoriasis model, myeloid and T cell populations were analyzed using the following antibodies: anti-mouse CD45 (clone 30-F11, BD Pharmingen), anti-mouse TCR β (clone H57-597, BD Horizon), anti-mouse TCR $\gamma\delta$ (clone GL3, BioLegend), anti-mouse CD4 (clone RM4-5, BD Horizon), anti-mouse CD8 α (clone 53-6.7, BioLegend), and anti-human CCR6 (clone G034E3, BioLegend). Dead cells were excluded using 7-AAD (BD Pharmingen).

In the CIA model, surface staining of myeloid and T cell populations was performed using the following antibodies: anti-mouse CD45 (clone 30-F11, BD Pharmingen), anti-mouse TCR β (clone H57-597, BD Horizon), anti-mouse TCR $\gamma\delta$ (clone GL3, BioLegend), anti-mouse CD4 (clone RM4-5, BD Horizon), anti-mouse CD8 α (clone 53-6.7, BioLegend), anti-mouse CD19 (clone 1D3, BD Pharmingen), anti-mouse Ly-6G (clone 1A8, BioLegend), anti-mouse CD11b (clone M1/70, BioLegend), anti-mouse NK-1.1 (clone PK136, BD Horizon), and anti-mouse F4/80 (clone T45-2342, BD OptiBuild). Dead cells were excluded using the fixable viability stain 620 (BD Horizon).

For intracellular cytokine analyses, cells were stimulated *ex vivo* with 2 μ L/mL cell stimulation cocktail (Tonbo Biosciences) for 4 hrs at 37 °C. Following stimulation, cells were washed with FACS buffer, fixed and permeabilized with BD fixation/permeabilization solution (BD Biosciences) in the dark at 4°C for 20 mins. Cells were

then washed with FACS buffer and intracellularly stained with anti-mouse IL-17A (clone TC11-18H10.1, BioLegend) and anti-mouse IFN- γ (clone XMG1.2, BioLegend) in the dark at 4°C for 30 minutes. Dead cells were excluded using the fixable viability stain 620 (BD Horizon). Cell counts were determined using CountBright absolute counting beads (Life Technologies) following the manufacturer's instructions. Flow cytometry data were acquired on a BD LSRFortessa X-20 (BD Biosciences) and analyzed using FlowJo software v10 (FlowJo, LLC).

2.11 Statistics

Data analysis and all graphical representations were performed using Prism 10.6.0 (GraphPad Software). Quantitative data were presented as mean \pm standard error of the mean. Comparison between multiple groups was analyzed using two-way analysis of variance or one-way analysis of variance followed by Tukey's multiple comparison test. Statistical significance was defined as a p-value of <0.05.

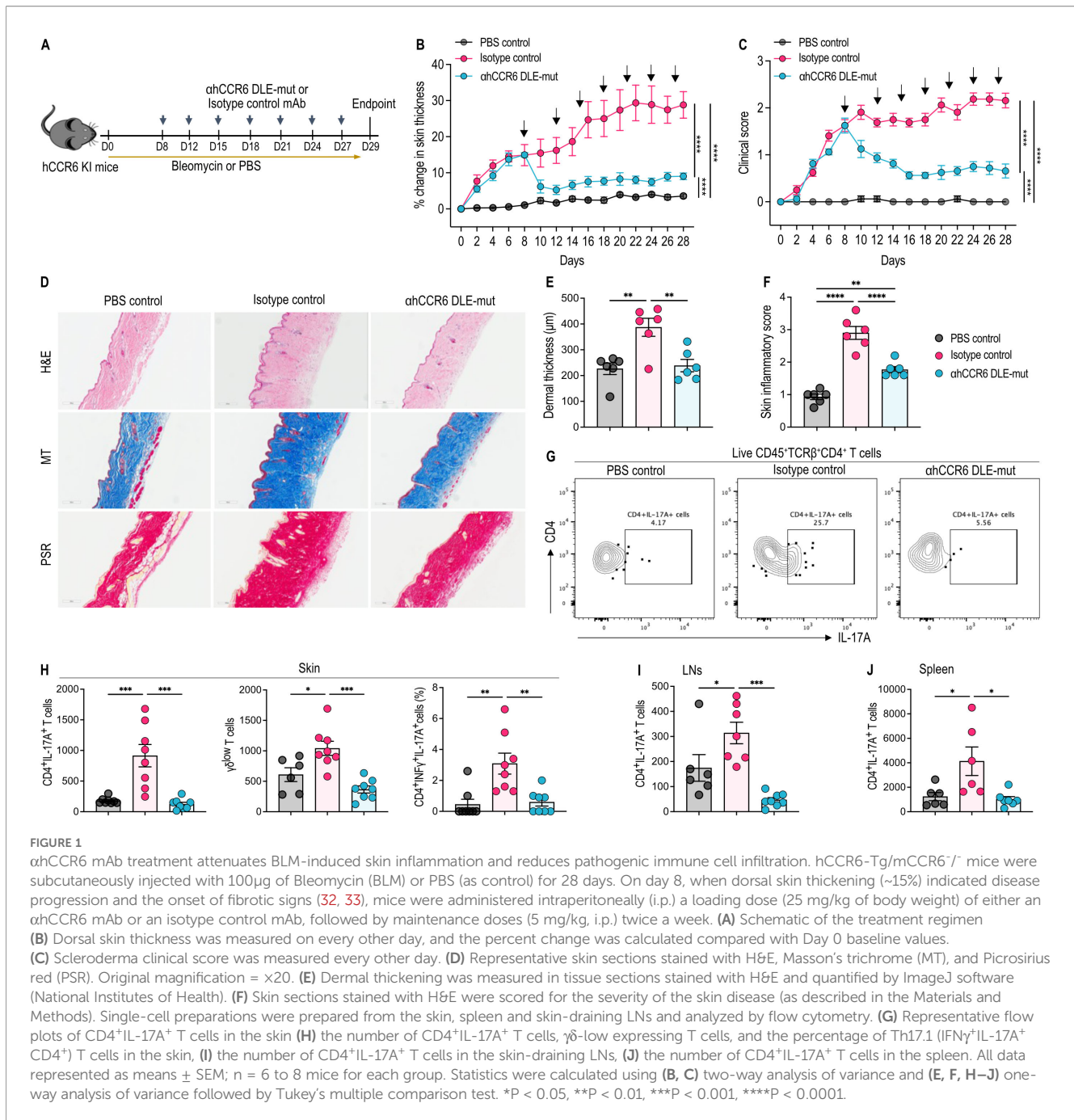
3 Results

3.1 α hCCR6 mAb attenuates skin inflammation and fibrosis by limiting pathogenic immune cell infiltration in a BLM-induced scleroderma model

To assess the therapeutic efficacy of Fc-enhanced α hCCR6 mAb in modulating fibrotic disease, we employed a bleomycin (BLM)-induced scleroderma model in human CCR6 knock-in (hCCR6 KI) mice. Subcutaneous BLM administration over four weeks induced hallmark features of scleroderma, including progressive dermal thickening, collagen deposition, and immune cell infiltration, closely mimicking the human disease phenotype (37). Treatment with α hCCR6 mAb was started on day 8, when displaying the onset of clinical symptoms (~15% increase in dorsal skin thickness and early fibrotic changes (32, 33) (Figures 1A, B).

In vitro characterization confirmed that our Fc-engineered α hCCR6 DLE-mut mAb exhibited potent, dose-dependent cytotoxicity against hCCR6⁺ target cells when co-incubated with human NK effector cells. Compared to the α hCCR6 Fc-Null (a CCR6-blocking antibody with a silenced Fc domain) and human IgG1 isotype control mAbs, α hCCR6 DLE-mut mAb significantly enhanced NK cell-mediated killing via ADCC mechanisms (Supplementary Figure S1).

Therapeutic administration of α hCCR6 DLE-mut mAb led to a marked reduction in dorsal skin thickness, a hallmark of skin inflammation and fibrosis, compared to isotype control-treated mice (Figure 1B). This was accompanied by a substantial decrease in cumulative clinical scores, which included assessments of skin thickening, erythema, and scaling (Figure 1C). Histopathological analysis of dorsal skin sections stained with H&E, MT, and PSR revealed that BLM injections markedly induced classic scleroderma



features, such as dermal thickening, excessive collagen deposition, loss of subcutaneous adipose tissue replaced by fibrotic matrix, and extensive leukocyte infiltration (Figures 1D–F). Remarkably, these pathological changes were substantially alleviated in mice treated with Fc-enhanced α hCCR6 mAb, indicating the therapeutic potential of this approach in limiting fibrotic and inflammatory responses.

In scleroderma, various immune cell subsets infiltrate into the target organs during the early stages of systemic fibrosis development (14, 36, 38). To further investigate the immunomodulatory effects of antibody treatment, we analyzed immune cell infiltration into affected tissues, including inflamed

skin, lung, skin-draining LNs, and the spleen, using flow cytometry. We observed that BLM injections markedly increased the numbers of various leukocyte populations in these sites, with a pronounced elevation of IL-17A-producing Th17 cells (CD4⁺IL-17A⁺ T cells) compared to PBS control (Figures 1G–J). Notably, α hCCR6 mAb treatment significantly reduced the number of pathogenic Th17 cell infiltrates compared to the isotype control (Figures 1G–J). BLM also elevated γ δ -low expressing T cells in the inflamed skin, a primary source of IL-17 during inflammation (9), which were effectively reduced by Fc-enhanced α hCCR6 mAb treatment. (Figure 1H).

Additionally, BLM administration significantly increased the total number of CD45⁺ leukocytes in the skin, skin-draining LNs,

and spleen (Supplementary Figures S2A–C). Our α hCCR6 mAb treatment led to a significant reduction in CD45⁺ cell numbers in the skin-draining LNs (Supplementary Figure S2B), whereas reductions in skin and spleen were not statistically significant (Supplementary Figures S2A, C). Importantly, α hCCR6 mAb treatment led to a significant decrease in CD4⁺ T cell numbers in the skin compared to isotype control, whereas other leukocyte subsets, including CD8⁺ T cells and neutrophils, remained unaffected (Supplementary Figure S2A). No significant differences were observed in the number of CD4⁺, CD8⁺, or $\gamma\delta$ T cell populations in LNs or spleen (Supplementary Figures S2B, C).

Interestingly, BLM induced an increase in the frequency of CD4⁺IFN γ ⁺IL-17A⁺ T cells (also known as Th17.1 cells) in the inflamed skin, whereas our α hCCR6 mAb significantly reduced this population compared to the isotype control (Figure 1H). Th17.1 cells represent a subset of Th17 cells that secrete both IL-17 and IFN- γ , thus playing a critical role in the pathogenesis of autoimmune diseases, including scleroderma (39–41).

These findings demonstrate that Fc-enhanced α hCCR6 mAb effectively limits fibrotic and inflammatory responses in the skin by selectively targeting CCR6⁺ pathogenic subsets, thereby attenuating scleroderma-associated inflammation.

3.2 α hCCR6 mAb inhibits lung inflammation and fibrosis through suppression of pathogenic immune cell recruitment in established BLM-induced scleroderma

Pulmonary fibrosis is a major complication in patients with scleroderma, and a leading cause of mortality in this population (42, 43). The BLM-induced scleroderma model also recapitulates key features of bronchoalveolar inflammation observed in humans, including lung fibrosis, alveolar damage, collagen deposition, and immune cell infiltration (36, 44).

Histological examination of lung tissue sections stained with H&E, MT, and PSR revealed severe pathological alterations in BLM-treated mice, including disruption of normal alveolar architecture, dense collagen deposition, and extensive leukocyte infiltration, compared to PBS control animals (Figure 2A). Treatment with the Fc-enhanced α hCCR6 mAb substantially reduced these pathological features, as reflected by lower lung inflammation and fibrosis scores compared with animals receiving an isotype control mAb (Figures 2B–D).

Flow cytometric analysis showed that BLM injections markedly increased the number of CD4⁺IL-17A⁺ Th17 cells and $\gamma\delta$ T cells in the lungs and lung-draining LNs of mice receiving isotype control mAb compared with PBS controls. Remarkably, α hCCR6 mAb treatment significantly decreased the abundance of these pathogenic immune subsets in these tissues (Figures 2E–G, and J). Similarly, BLM injections induced substantial infiltration of plasmacytoid dendritic cells (pDCs) into both the lung and lung-draining LNs, which was markedly reduced following α hCCR6 mAb treatment (Figures 2H, I). These cells play a crucial role in the development of

lung fibrosis by accumulating in the lungs and facilitating the recruitment of pathogenic immune cells to the affected tissues (36). However, their numbers remained unchanged in the spleen following BLM injections, indicating tissue-specific migration in response to BLM-induced inflammation (Figures 2H, I).

Although BLM injections also elevated total CD45⁺ leukocytes, CD4⁺, and CD8⁺ T cells in the lung, α hCCR6 mAb treatment did not significantly alter these populations (Supplementary Figure S2D). However, CD11c⁺CD11b⁺ myeloid dendritic cells (DCs) were elevated in both the lung and lung-draining LNs following BLM exposure, and α hCCR6 treatment selectively reduced their numbers in the LNs, while their numbers remained elevated in lung tissue (Supplementary Figures S2D, E). Similarly, total CD45⁺ leukocyte numbers were reduced in the LNs following α hCCR6 treatment but remained unchanged in lung tissue, while CD4⁺ and CD8⁺ T cells were unaffected at both sites (Supplementary Figures S2D, E).

Together, these results demonstrate that α hCCR6 mAb treatment suppresses lung inflammation and fibrosis by suppressing the recruitment of pathogenic Th17 cells, $\gamma\delta$ T cells, and pDCs, supporting the CCR6-targeted approach as a promising therapeutic strategy for pulmonary complications in scleroderma.

3.3 α hCCR6 mAb suppresses skin inflammation and reduces pathogenic immune cell infiltration in the IMQ-induced psoriasis model

Topical application of IMQ cream induces psoriatic skin inflammation in mice similar to human plaque-type psoriasis (45). To examine whether targeting CCR6⁺ cells alters disease severity, we administered Fc-enhanced anti-CCR6 mAb to IMQ-treated hCCR6 KI mice, which exhibited evident signs of the disease (~30% increase in dorsal skin thickening) on day 3 (Figures 3A, B).

Consistent with our previous findings using a CCR6-blocking mAb (13), treatment with the Fc-enhanced α hCCR6 mAb significantly alleviated disease symptoms in mice with established disease. This therapeutic benefit was evident through a substantial reduction in dorsal skin thickening, which serves as a surrogate marker of skin inflammation, as well as decreased skin redness and scaling compared to isotype control-treated animals (Figures 3B–D). Histopathological analysis further revealed that Fc-enhanced anti-CCR6 mAb exhibited marked suppression of hallmark features of psoriatic pathology, including acanthosis (epidermal thickening), parakeratosis, neutrophil microabscess formation, and dermal inflammatory infiltrates, compared to mice treated with an isotype control mAb (Figures 3E, F).

Additionally, Fc-enhanced anti-CCR6 mAb treatment significantly reduced the infiltration of inflammatory cells into the inflamed skin, including CD4⁺IL-17A⁺ Th17 cells, and $\gamma\delta$ -low expressing T cells, compared to mice treated with IMQ and receiving the isotype control mAb (Figures 3G–I). IMQ exposure also increased Th17 and $\gamma\delta$ T cells infiltration into the skin-draining LNs and spleen (Figures 3H, I). Th17 cells, which express high levels of CCR6 (1), play a central role in the pathogenesis of this disease

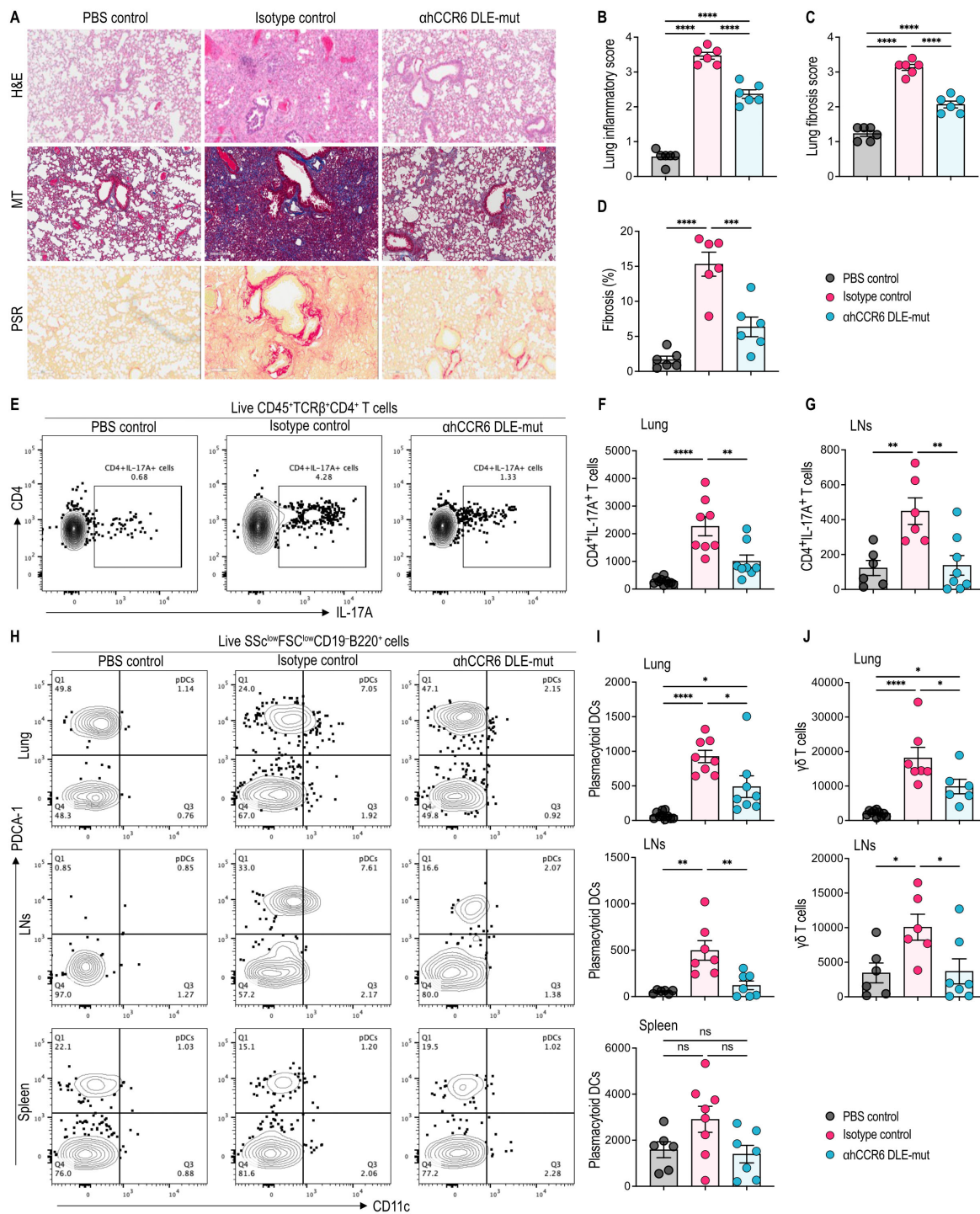
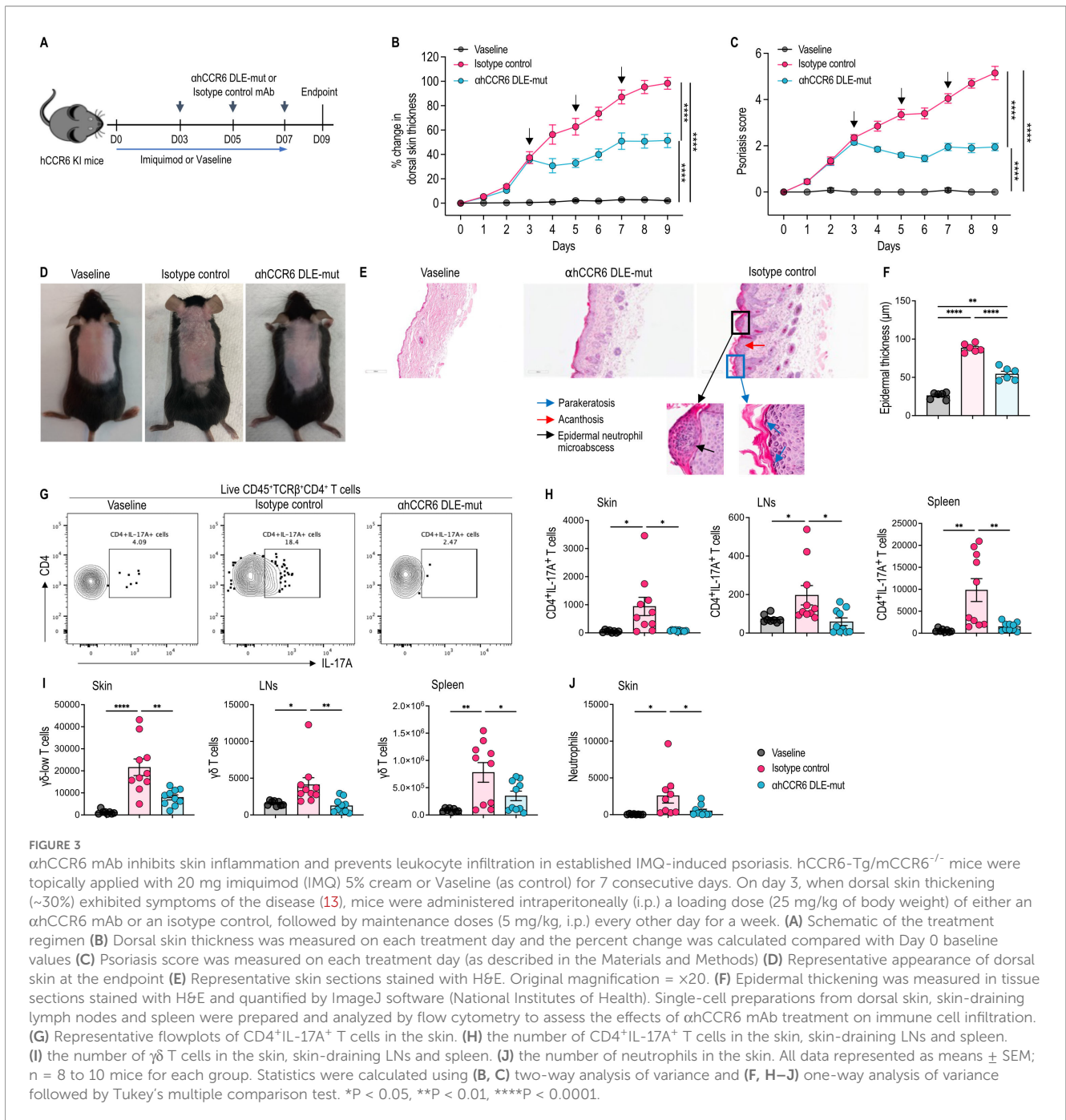


FIGURE 2
 α hCCR6 mAb treatment reduces BLM-induced lung inflammation, fibrosis and leukocyte infiltration. hCCR6-Tg/mCCR6^{-/-} mice were subcutaneously injected with 100 μ g of Bleomycin (BLM) or PBS (as control) for 28 days. On day 8, when dorsal skin thickening (~15%) indicated disease progression and the onset of fibrotic signs (32, 33), mice were administered intraperitoneally (i.p.) a loading dose (25 mg/kg of body weight) of either an α hCCR6 mAb or an isotype control mAb, followed by maintenance doses (5 mg/kg, i.p.) twice a week. **(A)** Representative lung tissue sections stained with H&E, Masson's trichrome (MT), and Picrosirius red (PSR). Original magnification = \times 20. **(B)** Lung tissue sections stained with H&E were scored for the severity of lung disease (as described in the Materials and Methods). **(C, D)** Lung tissue sections stained with MT were scored for fibrosis as the modified Ashcroft score (35, 36) (as described in Materials and Methods), and the percentage of lung fibrosis was quantified by ImageJ software (National Institutes of Health). Single-cell preparations were prepared from the lung, lung-draining LNs and spleen, and analyzed by flow cytometry. **(E)** Representative flowplots of CD4⁺IL-17A⁺ T cells in the lung. **(F, G)** the number of CD4⁺IL-17A⁺ T cells in the lung and lung-draining LNs. **(H)** Representative flow plots identifying plasmacytoid dendritic cells (pDCs) as live SSC^{low}FSC^{low}CD19⁺B220⁺ CD11c^{int}PDCA-1⁺ cells within the lymphocyte gate. **(I)** the number of pDCs infiltration in the lung, lung-draining LNs, and spleen. **(J)** the number of γ δ T cells in the lung and lung-draining LNs. All data represented as means \pm SEM; n = 6 to 8 mice for each group. Statistics were calculated using one-way analysis of variance followed by Tukey's multiple comparison test. *P < 0.05, **P < 0.01, ***P < 0.001, ****P < 0.0001.



(8, 13, 45, 46). In addition, $\gamma\delta$ -low T cells are a distinct dermal immune cell population (9) that serves as a major source of IL-17 during psoriatic skin inflammation and also express elevated levels of CCR6 (8, 10, 11). Notably, Fc-enhanced anti-CCR6 mAb treatment significantly reduced Th17 and $\gamma\delta$ T cell numbers in both the skin-draining LNs and spleen (Figures 3H, I). Likewise, neutrophil infiltration, a key driver of psoriatic pathology (47), was also significantly diminished in the skin following α hCCR6 treatment (Figure 3J).

Analysis of broader immune populations showed that the antibody treatment decreased total CD45⁺ leukocytes and CD4⁺

T cells in the skin, whereas CD8⁺ T cells and dendritic epidermal T cells (DETCs) remained unaffected (Supplementary Figure S3A). In contrast, CCR6 targeting did not significantly affect the infiltration of these immune cell populations in the skin-draining LNs or spleen (Supplementary Figure S3B, C).

These findings demonstrate that targeting of CCR6⁺ cells with α hCCR6 mAb effectively suppresses psoriatic inflammation by preventing infiltration of pathogenic Th17 cells, $\gamma\delta$ T cells, and neutrophils into inflamed tissues, underscoring the therapeutic promise of CCR6-targeted strategies for psoriasis and other IL-17/IL-22-driven diseases.

3.4 α hCCR6 mAb treatment alleviates disease severity in the collagen induced arthritis model

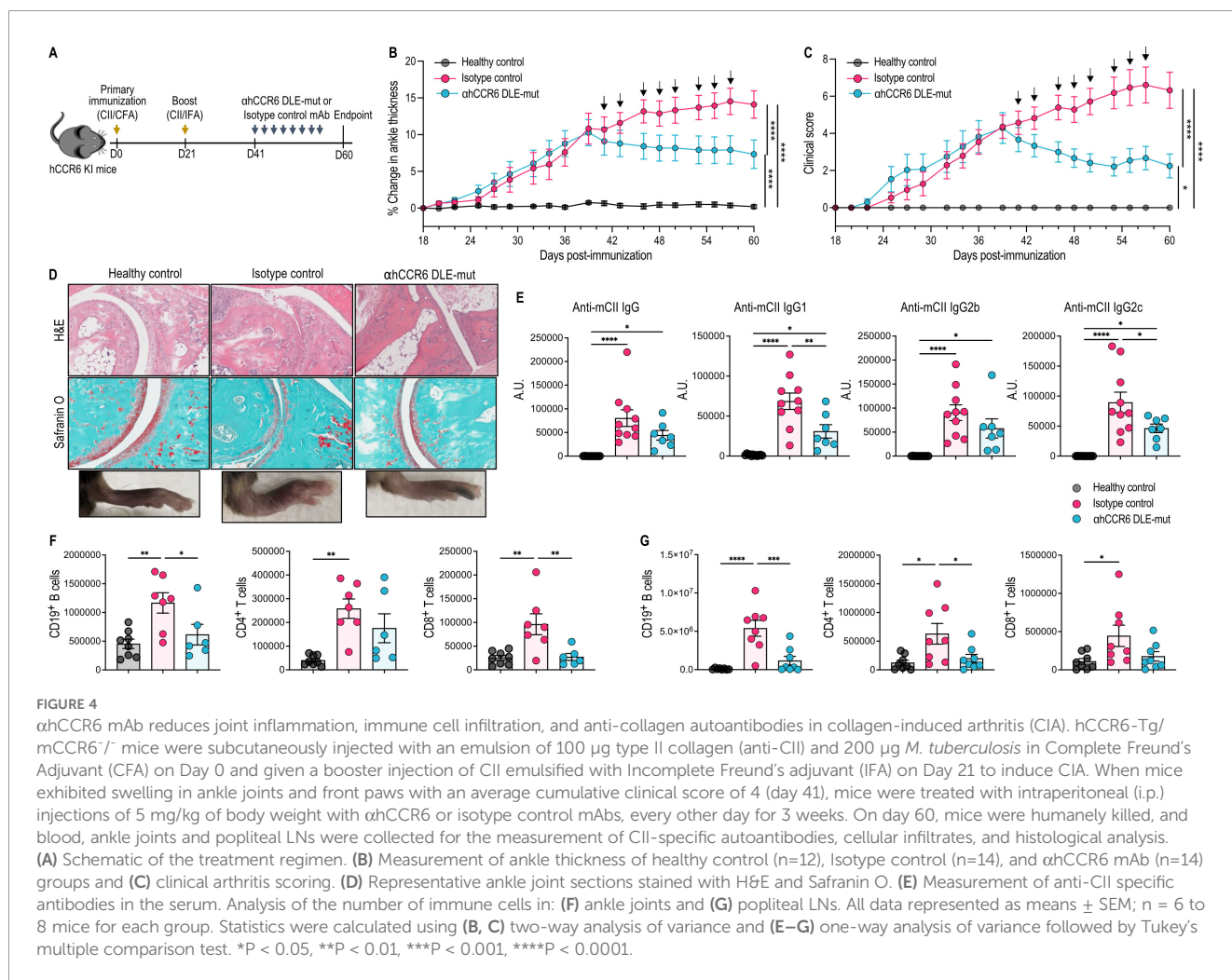
We further explored the therapeutic potential of targeting CCR6 using Fc-enhanced anti-CCR6 mAb treatment in another model of autoimmunity: the CIA model, a well-established model of autoimmune arthritis. In a therapeutic setting, the anti-CCR6 mAb was administered to hCCR6 KI mice with clinically evident CIA (average cumulative clinical score of 4 on day 41, characterized by swelling in the ankle joints and forepaws; Figures 4A–C). Our results showed that α hCCR6 mAb treatment significantly alleviated clinical symptoms of arthritis, as evidenced by reduced ankle thickening (a surrogate indicator of arthritis) and lower clinical scores, compared to the isotype control-treated animals (Figures 4B, C).

Histopathological assessment of the ankle joints confirmed these clinical improvements by displaying a notable reduction in inflammatory cell infiltration (as shown in H&E-stained sections) and preservation of normal joint structure, with minimal loss of cartilage proteoglycan at articular surfaces (as shown in Safranin O-stained sections), in the Fc-enhanced anti-

CCR6 mAb treated animals compared to the isotype control group (Figure 4D).

Considering the pathogenic role of anti-collagen type II (CII) antibodies in CIA, we measured circulating levels of anti-CII antibodies. These anti-CII-specific Abs are known to be arthritogenic and are essential for the development of CIA (48–50). We observed that α hCCR6 mAb treatment significantly reduced anti-CII-specific Ab titers, including anti-CII IgG1 and anti-CII IgG2c titers, compared to the isotype control, indicating attenuation of the pathogenic humoral response (Figure 4E).

Immune profiling of inflamed joints and popliteal draining LNs showed that α hCCR6 mAb significantly reduced the number of CD19⁺ B cells and CD8⁺ T cells in the joints, while CD4⁺ T cells remained unchanged (Figure 4F). In the draining LNs, α hCCR6 mAb reduced CD19⁺ B cells and CD4⁺ T cells, but not CD8⁺ T cells, when compared to mice treated with isotype control mAb (Figure 4G). Total CD45⁺ leukocytes and $\gamma\delta$ T cells numbers in the joints were unaffected, and although Th17 cell numbers trended lower, the reduction was not statistically significant (Supplementary Figure S4A). Infiltration of innate immune cells, including neutrophils, NK cells, and F4/80⁺ macrophages, was also unchanged in the joints (Supplementary Figure S4A). However, in



draining LNs, CCR6 targeting significantly reduced CD45⁺ leukocytes and $\gamma\delta$ T cells, but not Th17 cells (Supplementary Figure S4B).

Collectively, these results demonstrate that targeting CCR6⁺ cells using Fc-enhanced anti-CCR6 mAb treatment effectively alleviates CIA by dampening pathogenic anti-CII Abs responses and limiting infiltration of disease-associated immune cells into affected tissues. These findings underscore the role of CCR6⁺ immune cells in arthritis pathogenesis and support therapeutically targeting CCR6⁺ cells as a promising strategy for IL-17-driven autoimmune diseases.

4 Discussion

The migration of leukocytes to the site of inflammation is essential to innate immunity for host defense and maintaining immune homeostasis. Nevertheless, uncontrolled infiltration and activation of leukocytes into tissues can drive chronic inflammatory responses, leading to various pathologies, including autoimmune diseases. Among the key regulators of immune cell trafficking is the chemokine receptor CCR6, which is highly expressed on IL-17-producing Th17 cells and other pathogenic immune subsets and facilitates their directed migration to inflamed tissues, thus amplifying inflammatory responses and disease progression (1, 5–7). Consequently, antagonism or targeted depletion of this receptor holds considerable promise as an anti-inflammatory therapeutic strategy in inflammatory and autoimmune diseases. Numerous studies using CCR6-deficient mice or pharmacological inhibitors have demonstrated the critical role of this receptor in autoimmune and inflammatory disorders, leading to diminished inflammation in numerous animal models (1, 10, 26–28). Despite these therapeutic promises, no effective mAb against CCR6 has advanced to clinical studies (51), and only one small molecule inhibitor (PF-07054894) is currently undergoing phase 1 clinical trials (52). To address this gap, we have previously developed a fully humanized mAb against hCCR6 with potent antagonistic activity, which has shown efficacy in preclinical models of EAE and psoriasis (13).

Targeting CCR6 with mAb offers distinct advantages over neutralizing its ligand CCL20 due to the high levels of circulating CCL20, which can limit the efficacy of ligand-blocking strategies. Moreover, prior attempts to develop antibodies against CCL20 were halted after a Phase 1 trial due to immune complex-mediated toxicity observed in non-human primates (53). Furthermore, CCR6 binds to non-chemokine ligands, such as human β -defensin-1 and 2, which are upregulated during inflammation and contribute to the recruitment of Th17 cells to inflammation sites (54–56). These factors underscore the therapeutic rationale for directly targeting CCR6 rather than its ligands for treating inflammatory and autoimmune conditions. However, antagonizing chemokine receptors as a therapeutic approach has been quite disappointing, and only two small molecules against CXCR4 and CCR5 have been approved to date for human use.

In this study, we investigated the therapeutic efficacy of a Fc-enhanced anti-CCR6 mAb across multiple animal models of

autoimmunity: BLM-induced scleroderma, IMQ-induced psoriasis, and CIA. In the scleroderma model, therapeutic administration of α hCCR6 mAb resulted in a substantial reduction of skin inflammation and fibrosis, accompanied by a marked decrease in pathogenic immune cells, specifically IL-17-producing Th17 cells and Th17.1 cells, in the skin and skin-draining LNs. This observation following α hCCR6 mAb treatment highlights the critical role of CCR6⁺ cells in mediating inflammation, as well as the antibody's capacity to target highly pathogenic immune cell subsets. Studies in animal models and scleroderma patients have shown that Th17 cells contribute to the pathogenesis of this disease through the production of IL-17 (14, 21, 38, 57). Furthermore, Th17 cells secrete a spectrum of pro-inflammatory cytokines, including IFN- γ , IL-21 and IL-22 (58, 59). In alignment with this, we observed an increased frequency of IFN- γ -producing Th17.1 cells in the inflamed skin following BLM administration, and treatment with our Fc-enhanced anti-CCR6 mAb significantly diminished these inflammatory infiltrates. Th17.1 cells, a subset of Th17 cells, secrete both IL-17 and IFN- γ cytokines, thereby contributing critically to the pathogenesis of autoimmune diseases, including scleroderma (39–41). Previous studies have documented high levels of IL-17 and IFN- γ in the serum of scleroderma patients (39). A recent study reported a significant increase in the percentage of these Th17 cell subsets in the blood of scleroderma patients, facilitating fibroblast proliferation and collagen synthesis, which subsequently contributes to the dermal fibrosis observed in this condition (41). Additionally, we observed that selective targeting of CCR6 using the α hCCR6 mAb resulted in a marked reduction of $\gamma\delta$ -low T cells within the skin and skin-draining LNs. These cells exhibit higher levels of CCR6 (8) and are a major source of IL-17 (9, 12) during inflammation. These pathogenic subsets of $\gamma\delta$ T cells are known to migrate to inflamed tissues and contribute to disease progression through the production of high levels of Th17 cytokines (10, 12, 13).

Beyond cutaneous manifestations, BLM also induces lung inflammation and fibrosis (36, 44). In humans, pulmonary fibrosis is one of the main complications of scleroderma and is the leading cause of death among affected patients (42, 43). Remarkably, our α hCCR6 mAb significantly attenuated lung inflammation and fibrosis in the BLM-induced scleroderma model. This therapeutic benefit was associated with reduced infiltration of Th17 cells, $\gamma\delta$ T cells, and pDCs in both the lungs and lung-draining LNs. These cell types produce IL-17A (14, 38), TNF- α (60), and other pro-fibrotic mediators that drive lung inflammation and fibrosis (61, 62).

Interestingly, BLM injections selectively increase pDCs infiltration to the lungs and lung-draining LNs, but not the spleen, indicating targeted migration to affected tissues. These cells drive lung fibrosis by recruiting pathogenic immune cells and promoting pro-inflammatory and pro-fibrotic responses. Their reduction following mAb treatment reduces fibrosis and inflammatory infiltrates in both the skin and lungs (36). In scleroderma patients, elevated levels of pDCs in the lungs are associated with disease severity (36). pDCs infiltrate the lungs (63) and are potent producers of CXCL4 and

IFN- α , both of which are implicated in fibrotic responses and disease severity (64, 65).

While $\gamma\delta$ T cells are another key producer of IL-17A and known contributors to IL-17-mediated inflammation (66), their role in fibrosis is context-dependent. In some settings, their depletion may exacerbate disease, suggesting a dual role in immune regulation (67). Nonetheless, our data support their pathogenic contribution in the BLM model and highlight the therapeutic value of CCR6⁺ cell targeting.

In the psoriasis model, our Fc-enhanced anti-CCR6 mAb demonstrated robust therapeutic efficacy in suppressing psoriatic skin inflammation. Building on our previous work of antagonizing CCR6 using a CCR6-blocking mAb in a prophylactic setting of a preclinical model (13), this study evaluated the therapeutic potential of CCR6⁺ cell targeting with Fc-enhanced mAb after disease onset, which more closely reflects clinical treatment scenarios. Notably, the α hCCR6 mAb used here was not identical to that used in our earlier study: the current mAb was Fc-engineered to enhance binding affinity to both human and murine Fc γ receptors, thereby increasing ADCC and ADCP and enabling selective depletion of CCR6⁺ immune cells. By repeating the psoriasis experiment with this Fc-enhanced anti-CCR6 mAb, we directly assessed whether this new CCR6-targeted approach retains therapeutic potency under clinically relevant conditions. Thus, while our previous blocking antibody primarily interfered with CCR6–CCL20-driven migration, the Fc-enhanced α hCCR6 DLE-mut mAb additionally recruits Fc γ R-bearing effector cells and therefore has the potential to exert deeper and more sustained control of IL-17-driven inflammation than receptor blockade alone.

Treatment with α hCCR6 mAb demonstrated robust therapeutic benefits and significantly reduced hallmark features of psoriasis, such as skin thickening, erythema, and scaling. It also markedly decreased the infiltration of IL-17A-producing Th17 cells and $\gamma\delta$ -low T cells, key drivers of psoriatic pathology. These dermal $\gamma\delta$ T cells, which express high levels of CCR6, are the predominant source of IL-17 in murine psoriasis models and have human counterparts implicated in psoriatic lesions (8, 10, 11). In humans, an equivalent dermal $\gamma\delta$ T cell plays a similarly pathogenic role in psoriatic lesions (8). Our findings reinforce the therapeutic relevance of CCR6⁺ cell targeting and align with prior studies showing that genetic deletion or antibody-mediated blockade of CCR6 (13) or its ligand CCL20 (10) impairs disease development. These results validate α hCCR6 mAb as a promising candidate for psoriasis therapy and support broader application of CCR6-targeted strategies in other IL-17/IL-22-driven diseases.

In the CIA model, treatment with Fc-enhanced anti-CCR6 mAb effectively alleviated all clinical signs of arthritis, including reduced ankle swelling and lower cumulative disease scores. This therapeutic effect was accompanied by a reduction in circulating anti-CII IgG Abs and decreased infiltration of CD4⁺ and CD8⁺ T cells, as well as CD19⁺ B cells, into inflamed joints and draining LNs. These immune cell populations are central to RA pathogenesis (68–72) and frequently detected in the synovial fluid of RA patients (73–75). B cells, in particular, drive antigen-specific immune responses and contribute to disease progression through the production of rheumatoid factors and

high-affinity autoantibodies (73). Their deficiency or depletion using mAb treatment has been shown to prevent arthritis onset in murine models (76, 77). Furthermore, CII-specific antibodies are known to exacerbate joint inflammation and are key contributors to CIA (49, 78), highlighting the coordinated role of cellular and humoral immune responses in disease progression (79).

The observed reduction in anti-CII Ab titers following α hCCR6 mAb treatment suggests that CCR6-targeting may modulate the T–B cell axis, as reflected by reduced anti-CII antibody titers and diminished B-cell numbers in the joints and draining lymph nodes, although we did not directly enumerate CCR6⁺ B, Tfh or Treg cell populations in this study. CCR6 expression is transiently upregulated on activated B cells and influences germinal center dynamics, thereby impacting antibody production (4, 80). Moreover, CCR6⁺ Th17 and Th17.1 cells are known to provide potent B cell help via secretion of IL-21 and other cytokines (81, 82). By targeting CCR6⁺ cells with a Fc-enhanced anti-CCR6 mAb, we most likely disrupt this T–B cell axis, which in turn attenuates both cellular and humoral drivers of arthritis progression.

While our findings demonstrate the broad therapeutic potential of CCR6⁺ cell targeting with an Fc-enhanced anti-CCR6 mAb across multiple pre-established autoimmune disease models, a few limitations should be considered. First, our analyses focused primarily on Th17 cells, $\gamma\delta$ T cells, and pDCs, which are key drivers of autoimmune responses. However, we did not assess other CCR6⁺ populations, including B cells, innate lymphoid cells (ILCs), and plasma cells. In the CIA model, although we observed reduced anti-CII antibody levels due to the reduction of CCR6⁺ cells via Fc-enhanced mAb treatment, suggesting modulation of autoreactive B cell responses, a direct assessment of CCR6 expression on plasma cells is needed to confirm their involvement. Additionally, cytokine profiling in this study was limited to IL-17A and IFN- γ , and future studies should include other relevant mediators such as IL-22, TNF- α , and CCL20 to fully elucidate the immunological landscape. In addition, we did not perform dedicated pharmacokinetic and receptor occupancy in these models, and future translational work will need to define the relationships between exposure, target engagement, and modulation of CCR6-associated immune compartments.

Our findings demonstrate that therapeutic targeting of CCR6-expressing immune cells with an Fc-enhanced anti-CCR6 mAb is highly effective at reducing IL-17-driven inflammation across three pre-established autoimmune models. A limitation of our study is the lack of direct *in vivo* quantification of CCR6⁺ cells following antibody treatment. Indeed, the therapeutic antibody (clone 6H12) blocks the epitope recognized by available anti-CCR6 detection antibodies, precluding reliable staining of CCR6 after *in vivo* dosing. As a result, we infer engagement of CCR6⁺ targets indirectly from (i) robust NK-cell-mediated cytotoxicity *in vitro*, (ii) consistent reductions in IL-17-producing Th17 cells, $\gamma\delta$ -17 cells, pDCs, and B cells in inflamed tissues, and (iii) preservation of CCR6-negative leukocyte subsets. Altogether, these results highlight CCR6 as a central regulator of pathogenic immune cell trafficking and function, supporting the development of CCR6-targeted interventions for IL-17-driven autoimmune and inflammatory pathologies where current therapies remain inadequate.

Data availability statement

The raw data supporting the conclusions of this article will be made available by the authors, without undue reservation.

Ethics statement

The animal studies were reviewed and approved by the Animal Ethics Committee and Animal Welfare Committee of Monash University.

Author contributions

MA: Conceptualization, Project administration, Data curation, Formal Analysis, Investigation, Methodology, Validation, Visualization, Writing – original draft, Writing – review & editing. Y-AY: Data curation, Methodology, Visualization, Writing – review & editing. CA: Investigation, Methodology, Writing – review & editing. LX: Investigation, Methodology, Writing – review & editing. HS: Data curation, Writing – review & editing. CM: Conceptualization, Supervision, Writing – review & editing. RR: Conceptualization, Data curation, Funding acquisition, Project administration, Resources, Supervision, Writing – review & editing.

Funding

The author(s) declared that financial support was received for this work and/or its publication. This study was conducted as part of a collaborative effort between Monash University and Dragonfly Therapeutics, Inc., with Dragonfly Therapeutics, Inc. contributing funding to the study.

Acknowledgments

The authors acknowledge FlowCore and the Monash Histology Platform for their assistance with flow cytometry and histology analysis. The generation of the hCCR6-Tg/mCCR6-/knock-in mice used in this study was supported by the Australian Phenomics Network (APN) and the Australian Government through the National Collaborative Research Infrastructure Strategy (NCRIS) program.

Conflict of interest

HLS is employed by Dragonfly Therapeutics, Inc.

The remaining author(s) declared that this work was conducted in the absence of any commercial or financial relationships that could be construed as a potential conflict of interest. The author(s) declared that this work received funding from Dragonfly Therapeutics, Inc. The funder had the following involvement in

the study: study design, interpretation of data, and preparation of the manuscript.

Correction note

This article has been corrected with minor changes. These changes do not impact the scientific content of the article.

Generative AI statement

The author(s) declared that generative AI was used in the creation of this manuscript. Generative AI was used during the editing and proofreading process to check the structure, grammar and clarity of your writing.

Any alternative text (alt text) provided alongside figures in this article has been generated by Frontiers with the support of artificial intelligence and reasonable efforts have been made to ensure accuracy, including review by the authors wherever possible. If you identify any issues, please contact us.

Publisher's note

All claims expressed in this article are solely those of the authors and do not necessarily represent those of their affiliated organizations, or those of the publisher, the editors and the reviewers. Any product that may be evaluated in this article, or claim that may be made by its manufacturer, is not guaranteed or endorsed by the publisher.

Supplementary material

The Supplementary Material for this article can be found online at: <https://www.frontiersin.org/articles/10.3389/fimmu.2025.1728419/full#supplementary-material>

SUPPLEMENTARY FIGURE 1

Functional characterization of α hCCR6 mAb in NK cell-mediated cytotoxicity assay. Activated human natural killer (NK) cells (effector) were co-cultured with hCCR6-expressing L1.2 target cells at a fixed effector-to-target (E:T) ratio of 4:1. Cytotoxic activity was assessed *in vitro* using increasing concentrations of α hCCR6 DLE-mut, α hCCR6 Fc-Null, or human IgG1 isotype control mAbs. A dose-dependent enhancement of NK cell-mediated killing was observed with α hCCR6 DLE-mut mAb, demonstrating its functional potency and target specificity.

SUPPLEMENTARY FIGURE 2

Effect of α hCCR6 mAb on immune cell populations in the skin, lung, draining lymph nodes, and spleen of bleomycin (BLM)-treated mice. hCCR6-Tg/mCCR6^{-/-} mice were subcutaneously injected with 100 μ g of Bleomycin or PBS (as control) for 28 days. On day 8, when dorsal skin thickening (~15%) indicated disease progression, and the onset of fibrotic signs (32, 33), mice were administered intraperitoneally (i.p.) a loading dose (25 mg/kg of body weight) of either α hCCR6 or an isotype control mAbs, followed by maintenance doses (5 mg/kg, i.p.) twice a week. At the end of the experiment, single-cell preparations were prepared from the dorsal skin, spleen and skin-draining LNs and analyzed by flow cytometry. The effect of α hCCR6 mAb treatment on the number of leukocyte subsets infiltration was assessed in: (A) Dorsal skin, (B) skin-draining

LN, (C) Spleen, (D) Lung, and (E) Lung-draining LNs. All data represented as means \pm SEM; n = 6 to 8 mice for each group. Statistics were calculated using one-way analysis of variance followed by Tukey's multiple comparison test. *P < 0.05, **P < 0.01, ***P < 0.001, ****P < 0.0001.

SUPPLEMENTARY FIGURE 3

Effect of α hCCR6 mAb on immune cell subsets in the skin, skin-draining lymph nodes, and spleen of imiquimod (IMQ)-treated mice. hCCR6-Tg/mCCR6^{-/-} mice were topically applied with 20 mg imiquimod (IMQ) 5% cream or Vaseline (as control) for 7 consecutive days. On day 3, when dorsal skin thickening (~30%) indicated disease onset, mice were administered intraperitoneally (i.p.) a loading dose (25 mg/kg of body weight) of either α hCCR6 or an isotype control mAbs, followed by maintenance doses (5 mg/kg, i.p.) every other day for a week. At the end of the experiment, single-cell preparations were obtained from the dorsal skin, skin-draining LNs, and spleen and analyzed by flow cytometry. The effect of α hCCR6 mAb treatment on the number of leukocyte subsets infiltration were assessed in: (A) Dorsal skin, (B) skin-draining LNs, and (C) Spleen. All data represented as means \pm SEM; n = 8 to 10 mice for each group. Statistics were

calculated using one-way analysis of variance followed by Tukey's multiple comparison test. *P < 0.05, **P < 0.01, ***P < 0.001, ****P < 0.0001.

SUPPLEMENTARY FIGURE 4

Effect of α hCCR6 mAb on immune cell populations in the ankle and draining nodes in collagen-induced arthritis (CIA). hCCR6-Tg/mCCR6^{-/-} mice were subcutaneously injected with an emulsion of 100 μ g type II collagen (anti-CII) and 200 μ g *M. tuberculosis* in Complete Freund's Adjuvant (CFA) on Day 0 and given a booster injection of CII emulsified with Incomplete Freund's adjuvant (IFA) on Day 21 to induce CIA. When mice exhibited swelling in ankle joints and front paws with an average cumulative clinical score of 4 (day 41), mice were treated with intraperitoneal (i.p.) injections of 5 mg/kg of body weight with α hCCR6 or isotype control mAbs, every other day for 3 weeks. At the end of the experiment, single-cell preparations from the ankle and draining popliteal LNs were prepared and analyzed by flow cytometry. The effects of α hCCR6 mAb treatment on the number of leukocyte infiltrations were assessed in: (A) Ankle and (B) Draining popliteal LNs. All data represented as means \pm SEM; n = 6 to 8 mice for each group. Statistics were calculated using one-way analysis of variance followed by Tukey's multiple comparison test. *P < 0.05, **P < 0.01, ***P < 0.001, ****P < 0.0001.

References

- Hirota K, Yoshitomi H, Hashimoto M, Maeda S, Teradaira S, Sugimoto N, et al. Preferential recruitment of ccr6-expressing th17 cells to inflamed joints via ccl20 in rheumatoid arthritis and its animal model. *J Exp Med*. (2007) 204:2803–12. doi: 10.1084/jem.20071397
- Singh SP, Zhang HH, Foley JF, Hedrick MN, Farber JM. Human T cells that are able to produce il-17 express the chemokine receptor ccr6. *J Immunol*. (2008) 180:214–21. doi: 10.4049/jimmunol.180.1.214
- Lee AYS, Korner H. The ccr6-ccl20 axis in humoral immunity and T-B cell immunobiology. *Immunobiology*. (2019) 224:449–54. doi: 10.1016/j.imbio.2019.01.005
- Wiede F, Fromm PD, Comerford I, Kara E, Bannan J, Schuh W, et al. Ccr6 is transiently upregulated on B cells after activation and modulates the germinal center reaction in the mouse. *Immunol Cell Biol*. (2013) 91:335–9. doi: 10.1038/icb.2013.14
- Kim KE, Houh Y, Park HJ, Cho D. Therapeutic effects of erythroid differentiation regulator 1 on imiquimod-induced psoriasis-like skin inflammation. *Int J Mol Sci*. (2016) 17:244. doi: 10.3390/ijms17020244
- Lee AY, Korner H. Ccr6 and ccl20: emerging players in the pathogenesis of rheumatoid arthritis. *Immunol Cell Biol*. (2014) 92:354–8. doi: 10.1038/icb.2013.97
- Tao J, Li L, Tan Z, Li Y, Yang J, Tian F, et al. Up-regulation of cc chemokine ligand 20 and its receptor ccr6 in the lesional skin of early systemic sclerosis. *Eur J Dermatol*. (2011) 21:731–6. doi: 10.1684/ejd.2011.1469
- Cai Y, Shen X, Ding C, Qi C, Li K, Li X, et al. Pivotal role of dermal il-17-producing gammadelta T cells in skin inflammation. *Immunity*. (2011) 35:596–610. doi: 10.1016/j.immuni.2011.08.001
- Gray EE, Suzuki K, Cyster JG. Cutting edge: identification of a motile il-17-producing gammadelta T cell population in the dermis. *J Immunol*. (2011) 186:6091–5. doi: 10.4049/jimmunol.1100427
- Mabuchi T, Singh TP, Takekoshi T, Jia GF, Wu X, Kao MC, et al. Ccr6 is required for epidermal trafficking of gammadelta-T cells in an il-23-induced model of psoriasisform dermatitis. *J Invest Dermatol*. (2013) 133:164–71. doi: 10.1038/jid.2012.260
- Mabuchi T, Takekoshi T, Hwang ST. Epidermal ccr6+ Gammadelta T cells are major producers of il-22 and il-17 in a murine model of psoriasisform dermatitis. *J Immunol*. (2011) 187:5026–31. doi: 10.4049/jimmunol.1101817
- Haas JD, Gonzalez FH, Schmitz S, Chennupati V, Fohse L, Kremmer E, et al. Ccr6 and nk1.1 distinguish between il-17a and ifn-gamma-producing gammadelta effector T cells. *Eur J Immunol*. (2009) 39:3488–97. doi: 10.1002/eji.200939922
- Robert R, Ang C, Sun G, Juglair L, Lim EX, Mason LJ, et al. Essential role for ccr6 in certain inflammatory diseases demonstrated using specific antagonist and knockin mice. *JCI Insight*. (2017) 2. doi: 10.1172/jci.insight.94821
- Lei L, Zhong XN, He ZY, Zhao C, Sun XJ. Il-21 induction of cd4+ T cell differentiation into th17 cells contributes to bleomycin-induced fibrosis in mice. *Cell Biol Int*. (2015) 39:388–99. doi: 10.1002/cbin.10410
- Okamoto Y, Hasegawa M, Matsushita T, Hamaguchi Y, Huu DL, Iwakura Y, et al. Potential roles of interleukin-17a in the development of skin fibrosis in mice. *Arthritis Rheum*. (2012) 64:3726–35. doi: 10.1002/art.34643
- Fenoglio D, Battaglia F, Parodi A, Stringara S, Negrini S, Panico N, et al. Alteration of th17 and treg cell subpopulations co-exist in patients affected with systemic sclerosis. *Clin Immunol*. (2011) 139:249–57. doi: 10.1016/j.clim.2011.01.013
- Goncalves RSG, Pereira MC, Dantas AT, Almeida AR, Marques CDL, Rego M, et al. Il-17 and related cytokines involved in systemic sclerosis: perspectives. *Autoimmunity*. (2018) 51:1–9. doi: 10.1080/08916934.2017.1416467
- Kurasawa K, Hirose K, Sano H, Endo H, Shinkai H, Nawata Y, et al. Increased interleukin-17 production in patients with systemic sclerosis. *Arthritis Rheum*. (2000) 43:2455–63. doi: 10.1002/1529-0131(200011)43:11<2455::AID-ANR12>3.0.CO;2-K
- Mi S, Li Z, Yang HZ, Liu H, Wang JP, Ma YG, et al. Blocking il-17a promotes the resolution of pulmonary inflammation and fibrosis via tgfbeta1-dependent and -independent mechanisms. *J Immunol*. (2011) 187:3003–14. doi: 10.4049/jimmunol.1004081
- Wilson MS, Madala SK, Ramalingam TR, Gochuico BR, Rosas IO, Cheever AW, et al. Bleomycin and il-1beta-mediated pulmonary fibrosis is il-17a dependent. *J Exp Med*. (2010) 207:535–52. doi: 10.1084/jem.20092121
- Yang X, Yang J, Xing X, Wan L, Li M. Increased frequency of th17 cells in systemic sclerosis is related to disease activity and collagen overproduction. *Arthritis Res Ther*. (2014) 16:R4. doi: 10.1186/ar4430
- Leipe J, Grunke M, Dechant C, Reindl C, Kerzendorf U, Schulze-Koops H, et al. Role of th17 cells in human autoimmune arthritis. *Arthritis Rheum*. (2010) 62:2876–85. doi: 10.1002/art.27622
- Nistala K, Moncrieffe H, Newton KR, Varsani H, Hunter P, Wedderburn LR. Interleukin-17-producing T cells are enriched in the joints of children with arthritis, but have a reciprocal relationship to regulatory T cell numbers. *Arthritis Rheum*. (2008) 58:875–87. doi: 10.1002/art.23291
- van Hamburg JP, Asmawidjaja PS, Davelaar N, Mus AM, Colin EM, Hazes JM, et al. Th17 cells, but not th1 cells, from patients with early rheumatoid arthritis are potent inducers of matrix metalloproteinases and proinflammatory cytokines upon synovial fibroblast interaction, including autocrine interleukin-17a production. *Arthritis Rheum*. (2011) 63:73–83. doi: 10.1002/art.30093
- Corvaisier M, Delneste Y, Jeanvoine H, Preisser L, Blanchard S, Garo E, et al. Il-26 is overexpressed in rheumatoid arthritis and induces proinflammatory cytokine production and th17 cell generation. *PLoS Biol*. (2012) 10:e1001395. doi: 10.1371/journal.pbio.1001395
- Bracke KR, D'Hulst AI, Maes T, Moerloose KB, Demedts IK, Lebecque S, et al. Cigarette smoke-induced pulmonary inflammation and emphysema are attenuated in ccr6-deficient mice. *J Immunol*. (2006) 177:4350–9. doi: 10.4049/jimmunol.177.7.4350
- Chung SH, Chang SY, Lee HJ, Choi SH. The C-C chemokine receptor 6 (Ccr6) is crucial for th2-driven allergic conjunctivitis. *Clin Immunol*. (2015) 161:110–9. doi: 10.1016/j.clim.2015.08.004
- Liston A, Kohler RE, Townley S, Haylock-Jacobs S, Comerford I, Caon AC, et al. Inhibition of ccr6 function reduces the severity of experimental autoimmune encephalomyelitis via effects on the priming phase of the immune response. *J Immunol*. (2009) 182:3121–30. doi: 10.4049/jimmunol.0713169
- Kueh AJ, Pal M, Tai L, Liao Y, Smyth GK, Shi W, et al. An update on using crispr/cas9 in the one-cell stage mouse embryo for generating complex mutant alleles. *Cell Death Differ*. (2017) 24:1821–2. doi: 10.1038/cdd.2017.122
- Alam MJ, Xie L, Ang C, Fahimi F, Willingham SB, Kueh AJ, et al. Therapeutic blockade of ccr2 rapidly clears inflammation in arthritis and atopic dermatitis models: demonstration with surrogate and humanized antibodies. *MAbs*. (2020) 12:1856460. doi: 10.1080/19420862.2020.1856460
- Lee-MacAry AE, Ross EL, Davies D, Laylor R, Honeychurch J, Glennie MJ, et al. Development of a novel flow cytometric cell-mediated cytotoxicity assay using the fluorophores pkh-26 and to-pro-3 iodide. *J Immunol Methods*. (2001) 252:83–92. doi: 10.1016/s0022-1759(01)00336-2
- Artlett CM. Animal models of systemic sclerosis: their utility and limitations. *Open Access Rheumatol*. (2014) 6:65–81. doi: 10.2147/OARRR.S50009

33. Mor A, Segal Salto M, Katav A, Barashi N, Edelshtein V, Manetti M, et al. Blockade of ccl24 with a monoclonal antibody ameliorates experimental dermal and pulmonary fibrosis. *Ann Rheum Dis.* (2019) 78:1260–8. doi: 10.1136/annrheumdis-2019-215119
34. Inglis JJ, Simelyte E, McCann FE, Criado G, Williams RO. Protocol for the induction of arthritis in C57bl/6 mice. *Nat Protoc.* (2008) 3:612–8. doi: 10.1038/nprot.2008.19
35. Hubner RH, Gitter W, El Mokhtari NE, Mathiak M, Both M, Bolte H, et al. Standardized quantification of pulmonary fibrosis in histological samples. *Biotechniques.* (2008) 44:507–11. doi: 10.2144/000112729
36. Kafaja S, Valera I, Divekar AA, Saggarr R, Abtin F, Furst DE, et al. Pdc5 in lung and skin fibrosis in a bleomycin-induced model and patients with systemic sclerosis. *JCI Insight.* (2018) 3. doi: 10.1172/jci.insight.98380
37. Yamamoto T, Takagawa S, Katayama I, Yamazaki K, Hamazaki Y, Shinkai H, et al. Animal model of sclerotic skin. I. local injections of bleomycin induce sclerotic skin mimicking scleroderma. *J Invest Dermatol.* (1999) 112:456–62. doi: 10.1046/j.1523-1747.1999.00528.x
38. Lei L, Zhao C, Qin F, He ZY, Wang X, Zhong XN. Th17 cells and il-17 promote the skin and lung inflammation and fibrosis process in a bleomycin-induced murine model of systemic sclerosis. *Clin Exp Rheumatol.* (2016) 34 Suppl 100:14–22.
39. Balanescu P, Ladaru A, Balanescu E, Nicolau A, Baicus C, Dan GA. Il-17, il-6 and ifn-gamma in systemic sclerosis patients. *Rom J Intern Med.* (2015) 53:44–9. doi: 10.1515/rjim-2015-0006
40. Ramstein J, Broos CE, Simpson LJ, Ansel KM, Sun SA, Ho ME, et al. Ifn-gamma-producing T-helper 17.1 cells are increased in sarcoidosis and are more prevalent than T-helper type 1 cells. *Am J Respir Crit Care Med.* (2016) 193:1281–91. doi: 10.1164/rccm.201507-1499OC
41. Xing X, Li A, Tan H, Zhou Y. Ifn-gamma(+) il-17(+) th17 cells regulate fibrosis through secreting il-21 in systemic scleroderma. *J Cell Mol Med.* (2020) 24:13600–8. doi: 10.1111/jcmm.15266
42. Steen VD, Medsger TA Jr. Severe organ involvement in systemic sclerosis with diffuse scleroderma. *Arthritis Rheum.* (2000) 43:2437–44. doi: 10.1002/1529-0131(200011)43:11<2437::AID-ANR10>3.0.CO;2-U
43. Steen VD, Medsger TA. Changes in causes of death in systemic sclerosis, 1972–2002. *Ann Rheum Dis.* (2007) 66:940–4. doi: 10.1136/ard.2006.066068
44. Yoshizaki A, Iwata Y, Komura K, Ogawa F, Hara T, Muroi E, et al. Cd19 regulates skin and lung fibrosis via toll-like receptor signaling in a model of bleomycin-induced scleroderma. *Am J Pathol.* (2008) 172:1650–63. doi: 10.2353/ajpath.2008.071049
45. van der Fits L, Mourits S, Voerman JS, Kant M, Boon L, Laman JD, et al. Imiquimod-induced psoriasis-like skin inflammation in mice is mediated via the il-23/il-17 axis. *J Immunol.* (2009) 182:5836–45. doi: 10.4049/jimmunol.0802999
46. Benham H, Norris P, Goodall J, Wechalekar MD, FitzGerald O, Szentpetery A, et al. Th17 and th22 cells in psoriatic arthritis and psoriasis. *Arthritis Res Ther.* (2013) 15:R136. doi: 10.1186/ar4317
47. Sumida H, Yanagida K, Kita Y, Abe J, Matsushima K, Nakamura M, et al. Interplay between cxcr2 and blt1 facilitates neutrophil infiltration and resultant keratinocyte activation in a murine model of imiquimod-induced psoriasis. *J Immunol.* (2014) 192:4361–9. doi: 10.4049/jimmunol.1302959
48. Nandakumar KS, Backlund J, Vestberg M, Holmdahl R. Collagen type ii (Cii)-specific antibodies induce arthritis in the absence of T or B cells but the arthritis progression is enhanced by cii-reactive T cells. *Arthritis Res Ther.* (2004) 6:R544–50. doi: 10.1186/ar1217
49. Stuart JM, Dixon FJ. Serum transfer of collagen-induced arthritis in mice. *J Exp Med.* (1983) 158:378–92. doi: 10.1084/jem.158.2.378
50. Trentham DE, Townes AS, Kang AH, David JR. Humoral and cellular sensitivity to collagen in type ii collagen-induced arthritis in rats. *J Clin Invest.* (1978) 61:89–96. doi: 10.1172/JCI108929
51. Hutchings CJ. A review of antibody-based therapeutics targeting G protein-coupled receptors: an update. *Expert Opin Biol Ther.* (2020) 20:925–35. doi: 10.1080/14712598.2020.1745770
52. Pfizer. *Study of single and multiple ascending doses of pf-07054894 in healthy adult participants.* ClinicalTrials.gov ID NCT04388878 (2020). Available online at: <https://clinicaltrials.gov/study/NCT04388878> (Accessed April 11, 2025).
53. Laffan SB, Thomson AS, Mai S, Fishman C, Kambara T, Nistala K, et al. Immune complex disease in a chronic monkey study with a humanised, therapeutic antibody against ccl20 is associated with complement-containing drug aggregates. *PLoS One.* (2020) 15:e0231655. doi: 10.1371/journal.pone.0231655
54. Ghannam S, Dejou C, Pedretti N, Giot JP, Dorgham K, Boukhaddaoui H, et al. Ccl20 and beta-defensin-2 induce arrest of human th17 cells on inflamed endothelium *in vitro* under flow conditions. *J Immunol.* (2011) 186:1411–20. doi: 10.4049/jimmunol.1000597
55. Hollox EJ, Huffmeier U, Zeeuwen PL, Palla R, Lascorz J, Rodijk-Oldhuis D, et al. Psoriasis is associated with increased beta-defensin genomic copy number. *Nat Genet.* (2008) 40:23–5. doi: 10.1038/ng.2007.48
56. Yang D, Chertov O, Bykovskaia SN, Chen Q, Buffo MJ, Shogan J, et al. Beta-defensins: linking innate and adaptive immunity through dendritic and T cell ccr6. *Science.* (1999) 286:525–8. doi: 10.1126/science.286.5439.525
57. Olewicz-Gawlik A, Danczak-Pazdrowska A, Kuznar-Kaminska B, Gornowicz-Porowska J, Katulska K, Trzybulska D, et al. Interleukin-17 and interleukin-23: importance in the pathogenesis of lung impairment in patients with systemic sclerosis. *Int J Rheum Dis.* (2014) 17:664–70. doi: 10.1111/1756-185X.12290
58. Feng S, Chen XM, Wang JF, Xu XQ. Th17 cells associated cytokines and cancer. *Eur Rev Med Pharmacol Sci.* (2016) 20:4032–40.
59. Ouyang W, Kolls JK, Zheng Y. The biological functions of T helper 17 cell effector cytokines in inflammation. *Immunity.* (2008) 28:454–67. doi: 10.1016/j.immuni.2008.03.004
60. Langrish CL, Chen Y, Blumenschein WM, Mattson J, Basham B, Sedgwick JD, et al. Il-23 drives a pathogenic T cell population that induces autoimmune inflammation. *J Exp Med.* (2005) 201:233–40. doi: 10.1084/jem.20041257
61. Libura J, Bettens F, Radkowski A, Tiercy JM, Piguat PF. Risk of chemotherapy-induced pulmonary fibrosis is associated with polymorphic tumour necrosis factor-A2 gene. *Eur Respir J.* (2002) 19:912–8. doi: 10.1183/09031936.02.00238102
62. Riha RL, Yang IA, Rabnott GC, Tunnicliffe AM, Fong KM, Zimmerman PV. Cytokine gene polymorphisms in idiopathic pulmonary fibrosis. *Intern Med J.* (2004) 34:126–9. doi: 10.1111/j.1444-0903.2004.00503.x
63. Divekar A, Khanna D, Abtin F, Maranian P, Saggarr R, Saggarr R, et al. Pdc5 and il-4+ T-cells in scleroderma as novel targets of imatinib mesylate. *J Immunol.* (2011) 186:44.18. doi: 10.4049/jimmunol.186.Supp.44.18
64. Ah Kioon MD, Tripodo C, Fernandez D, Kirou KA, Spiera RF, Crow MK, et al. Plasmacytoid dendritic cells promote systemic sclerosis with a key role for tlr8. *Sci Transl Med.* (2018) 10. doi: 10.1126/scitranslmed.aam8458
65. van Bon L, Affandi AJ, Broen J, Christmann RB, Marijnissen RJ, Stawski L, et al. Proteome-wide analysis and cxcl4 as a biomarker in systemic sclerosis. *N Engl J Med.* (2014) 370:433–43. doi: 10.1056/NEJMoa1114576
66. Lo Re S, Dumoutier L, Couillin I, Van Vyve C, Yakoub Y, Uwambayinema F, et al. Il-17a-producing gammadelta T and th17 lymphocytes mediate lung inflammation but not fibrosis in experimental silicosis. *J Immunol.* (2010) 184:6367–77. doi: 10.4049/jimmunol.0900459
67. Senoo S, Higo H, Taniguchi A, Kiura K, Maeda Y, Miyahara N. Pulmonary fibrosis and type-17 immunity. *Respir Investig.* (2023) 61:553–62. doi: 10.1016/j.resinv.2023.05.005
68. Berek C, Kim HJ. B-cell activation and development within chronically inflamed synovium in rheumatoid and reactive arthritis. *Semin Immunol.* (1997) 9:261–8. doi: 10.1006/smim.1997.0076
69. Corthay A, Johansson A, Vestberg M, Holmdahl R. Collagen-induced arthritis development requires alpha beta T cells but not gamma delta T cells: studies with T cell-deficient (Tcr mutant) mice. *Int Immunol.* (1999) 11:1065–73. doi: 10.1093/intimm/11.7.1065
70. Moder KG, Luthra HS, Kubo R, Griffiths M, David CS. Prevention of collagen induced arthritis in mice by treatment with an antibody directed against the T cell receptor alpha beta framework. *Autoimmunity.* (1992) 11:219–24. doi: 10.3109/08916939209035158
71. Strober S, Holoshitz J. Mechanisms of immune injury in rheumatoid arthritis: evidence for the involvement of T cells and heat-shock protein. *Immunol Rev.* (1990) 118:233–55. doi: 10.1111/j.1600-065x.1990.tb00818.x
72. Taneja V, Krco CJ, Behrens MD, Luthra HS, Griffiths MM, David CS. B cells are important as antigen presenting cells for induction of mhc-restricted arthritis in transgenic mice. *Mol Immunol.* (2007) 44:2988–96. doi: 10.1016/j.molimm.2006.12.026
73. Kim HJ, Berek C. B cells in rheumatoid arthritis. *Arthritis Res.* (2000) 2:126–31. doi: 10.1186/ar77
74. Van Boxel JA, Paget SA. Predominantly T-cell infiltrate in rheumatoid synovial membranes. *N Engl J Med.* (1975) 293:517–20. doi: 10.1056/NEJM197509112931101
75. He X, Kang AH, Stuart JM. Anti-human type ii collagen cd19+ B cells are present in patients with rheumatoid arthritis and healthy individuals. *J Rheumatol.* (2001) 28:2168–75.
76. Svensson L, Jirholt J, Holmdahl R, Jansson L. B cell-deficient mice do not develop type ii collagen-induced arthritis (Cia). *Clin Exp Immunol.* (1998) 111:521–6. doi: 10.1046/j.1365-2249.1998.00529.x
77. Dunussi-Joannopoulos K, Hancock GE, Kunz A, Hegen M, Zhou XX, Sheppard BJ, et al. B-cell depletion inhibits arthritis in a collagen-induced arthritis (Cia) model, but does not adversely affect humoral responses in a respiratory syncytial virus (Rsv) vaccination model. *Blood.* (2005) 106:2235–43. doi: 10.1182/blood-2004-11-4547
78. Watson WC, Brown PS, Pitcock JA, Townes AS. Passive transfer studies with type ii collagen antibody in B10.D2/old and new line and C57bl/6 normal and beige (Chediak-higashi) strains: evidence of important roles for C5 and multiple inflammatory cell types in the development of erosive arthritis. *Arthritis Rheum.* (1987) 30:460–5. doi: 10.1002/art.1780300418
79. Seki N, Sudo Y, Yoshioka T, Sugihara S, Fujitsu T, Sakuma S, et al. Type ii collagen-induced murine arthritis. I. Induction and perpetuation of arthritis require synergy between humoral and cell-mediated immunity. *J Immunol.* (1988) 140:1477–84. doi: 10.4049/jimmunol.140.5.1477
80. Reimer D, Lee AY, Bannan J, Fromm P, Kara EE, Comerford I, et al. Early ccr6 expression on B cells modulates germinal centre kinetics and efficient antibody responses. *Immunol Cell Biol.* (2017) 95:33–41. doi: 10.1038/icb.2016.68
81. Kim Y, Manara F, Grassmann S, Belcheva KT, Reyes K, Kim H, et al. Il-21 shapes the B cell response in a context-dependent manner. *Cell Rep.* (2025) 44:115190. doi: 10.1016/j.celrep.2024.115190
82. Quast I, Dvorscek AR, Pattaroni C, Steiner TM, McKenzie CI, Pitt C, et al. Interleukin-21, acting beyond the immunological synapse, independently controls T follicular helper and germinal center B cells. *Immunity.* (2022) 55:1414–30 e5. doi: 10.1016/j.immuni.2022.06.020